American Journal of Nanosciences
2022; 8(1): 8-12
http://www.sciencepublishinggroup.com/j/ajn
doi: 10.11648/j.ajn.20220801.12
ISSN: 2575-484X (Print); ISSN: 2575-4858 (Online)

Many-Body Interactions on Phonon Properties of Stanene

Kamlesh Kumar, Mohammad Imran Aziz*

Physics Department, Shibli National Postgraduate College, Azamgarh, India

Email address:
azizimran33@gmail.com (M. I. Aziz)
*Corresponding author

To cite this article:
Kamlesh Kumar, Mohammad Imran Aziz. Many-body Interactions on Phonon Properties of Stanene. *American Journal of Nanosciences*. Vol. 8, No. 1, 2022, pp. 8-12. doi: 10.11648/j.ajn.20220801.12

Received: April 20, 2022; **Accepted**: May 5, 2022; **Published**: May 12, 2022

Abstract: Novel properties are observed to arise at 2d level, which is typically absent in their bulk counterparts. Graphene, the most widely studied 2D material. Recently, the other 2D group-IV materials, silicene, germanene and stanene, have been realized by epitaxial growth on substrates and attracted tremendous interest due to their extraordinary properties. The discovery of stanene, a buckled monolayer of tin atoms arranged in a 2D honeycomb lattice, has explored enormous research interest in the materials in the two-dimensional (2D) realm. Stanene exhibit ductile nature and hence could be easily incorporated with existing technology in semiconductor industry on substrates in comparison to Graphene. the systematic investigation of phonon properties for stanene is needed. The general three dimensional continuum model of phonons in two dimensional materials is developed. At present, our research group find the lattice dynamical matrix and secular equations with solutions, phonon dispersion curve and Phonon density of states using Adiabatic Bond Charge Model with the help of MATLAB. We hope that phonon properties of Stanene will be good fitted with experimental data.

Keywords: Many-Body Interactions, Adiabatic Bond Charge Model, Phonon, Stanene as a 2D Material

1. Introduction

The atoms in a solid are executing oscillations about their equilibrium positions with energy governed by the temperature of the solid. Such oscillations in crystals are called lattice vibrations. The lattice vibrations are responsible for the characteristic properties of matter such as specific heat, thermal conductivity, electrical conductivity, optical, elastic, dielectric properties, diffusion mechanism, phase change phenomena etc. The vibration of the atoms depends on the interatomic interaction within the crystal. To determine the vibrational frequencies and the corresponding modes one needs to calculate the eigenvalues and the eigenvectors of the so-called dynamical matrix, which can be obtained from the interatomic interactions potential [7-10]. If the dynamical matrix is known, the eigenvalues problem is straightforward. There have been several theoretical attempts to understand the lattice vibrations and Phonon properties of Stanene [11-13] usually employing the force constant model, the rigid ion model, the rigid shell model, the dipole approximation etc, but bond charge model is showing best results for IV th group of semiconductor. The experimental and theoretical studies on grapheme created significant interest in on other Group IV elements, compound of III-V and II-VI Group compound 2D nanostructures. Very recently, we have reported that among Group IV elements, not only C but also Si, Ge and Sn can form stable honeycomb structures [1-5]. The adiabatic bond charge (BCM) method was originally developed by Weber [3] in 1976. For studying the lattice dynamics of tetrahedrally bonded bulk group- IV semi conductors such as Silicon Germanium and Diamond. The model was also adapted by Rustagi and Weber for studying III- V Semiconductor [4] such as Gallium Arsenide. In Weber's approach the atom is considered a non- polarizable ion Core and a shell of Valence electrons. The Valence Charge density is considered as point charges, called bond charges which are located midway (For homopolar case) along the tetrahedral bonds between the nearest neighbors, whereas for (hetero polar) III-V semiconductors they are nearer to the anions. These bond Charges are allowed to move adiabatically and are assumed to have zero mass. The equations of motion for the ions and their bond charges are evaluated and a dynamical matrix is obtained by considering three type of Interaction (i) Coulomb interactions (ii) Short

range central force Interactions and (iii) a rotationally invariant Keating type bond bending Interaction depending on angle. These interactions are depicted in Figure 1.

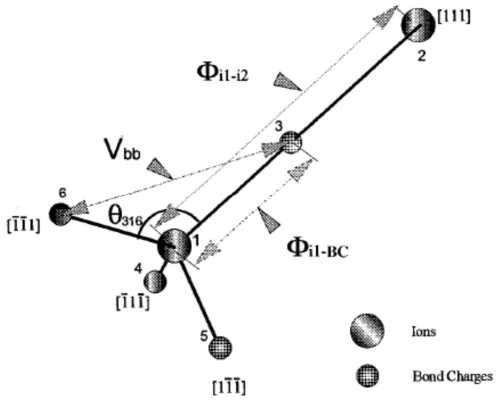

Figure 1. *Structure of unit cell and the interactions in the bond-charge model.*

Metal-like bonding is represented by the short-range central forces between ions $\left(\Phi_{i1-i2}\right)$ and covalent bonding is represented by the with cations and anions, and form interaction (c) there are different force constants associated with the BC-cation-BC and BC-anion-BC angles Keating interactions between the BC's (V_{bb}). For interaction (b) there are separate terms due to the interactions of the bond charges.

2. Modified Adiabatic Bond Charge Model

The two-dimensional honeycomb lattice (Figure 2) is

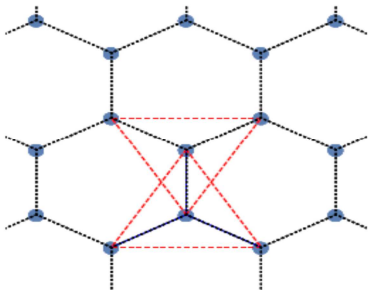

Figure 2. *Stanene Lattice.*

The honeycomb 2D structure contains two ions and three BCs. Thus the magnitude of BCs is -2Ze and +3ze magnitude of ions due to neutrality of crystals. According to adiabatic bond charge model, there are three type of Interactions (i) Coulomb interactions (ii) Short range central force Interactions and (iii) a rotationally invariant Keating type bond bending Interaction depending on angle. In calculation of total potential energy, we added the zero point energy [5-6]. Moreover, with a finite nanocrystal, the Ewald transformation cannot be applied anymore but finite summations have to be computed.

The total energy per unit cell of honeycomb structure is

$$\Phi_{total}=3\left[\varphi_{ii}(t)+\varphi_1(r_1)+\varphi_2(r_2)\right]-\alpha^{eff}{}_M\frac{(3Z)^2e^2}{\varepsilon t}+3\left[V^1_{bb}+V^2_{bb}+\psi_1\left(r^1{}_{bb}\right)+\psi_2\left(r^2{}_{bb}\right)\right]+\frac{1}{2}hw_j(q) \quad (1)$$

In homopolar crystal $\Phi_1(r_1)=\Phi_2(r_2)$ and $V^1_{bb}=V^2_{bb}$. In addition, the ions and the BCs interact via the Coulomb interaction characterized by single parameter Z^2/ε where -2Ze is the charge of BC, and ε is the dielectric constant.

To reduce the number of parameters it is assumed that $\psi'_1=\psi'_2$ =0, $\psi''=-\psi''=(B_2-B_2)/8$ and $(1+p)\Phi'_1+(1-p)\Phi'_2=0$ along the conditions for minimization of total energy per unit cell, which are $\left(\frac{\partial\Phi}{\partial t}\right)_0=0$ and $\left(\frac{\partial\Phi}{\partial p}\right)_0=0$ leads to

$$\varphi'_{ii}=-\alpha_m\frac{Z^2}{\varepsilon}\frac{e^2}{t}$$

$$\frac{\varphi'_1}{r_1}=2\frac{d\alpha_m}{dp}\frac{1-p}{1+p}\frac{Z^2}{\varepsilon}\frac{e^2}{t^3} \quad (2)$$

$$\frac{\varphi'_2}{r_2}=-2\frac{d\alpha_m}{dp}\frac{1+p}{1-p}\frac{z^2}{\varepsilon}\frac{e^2}{t^3}$$

The six parameters of the model are $\varphi''_{ii},\varphi''_1,\varphi''_2,B_1,B_2,$ and z^2/ε (Four for homopolar crystal).

The Fourier transformed of modified adiabatic bond Charge Model equations of motion.

$$m\omega^2u=\left[R+9\frac{(Ze)^2}{\varepsilon}C_R\right]u+\left[T-6\frac{(Ze)^2}{\varepsilon}C_T\right]v \quad (3)$$

$$0=\left[T^+-6\frac{(Ze)^2}{\varepsilon}C_T{}^+\right]u+\left[S+4\frac{(Ze)^2}{\varepsilon}C_S\right]v\ldots\ldots.$$

The above equations the $D_{\alpha\beta}(kk';q)$ can be reduced the ions the bond charge move adiabatically this gives.

$$D^{eff}=D^{ion-ion}-\left[D^{BC-ion}\right]^*\left[D^{BC-BC}\right]^{-1}\left[D^{BC-ion}\right]$$

Where the D,^{s} are those parts of the dynamical matrix referenced by their superscript and * denotes Hermitian conjugates. The condition for the non-trival solutions for wave amplitudes of Eq. 3 lead to the characteristic or secular

equation,

$$\left|D^{eff}(q)-\omega^2(q)mI\right|=0 \quad (4)$$

$$\omega=\omega_j(q);\ j=1,2,3,.....2n$$

This is the secular equation of 2x2 dimensions. Further it can be further extended as

$$-\omega^2 m_1 U=[D(0,0)-+D(0,1)D(1,1)^{-1}D(1,0)]U$$

where

$$D(0,0)=\begin{pmatrix}D_{xx}(0,0) & D_{xy}(0,0)\\ D_{yx}(0,0) & D_{yy}(0,0)\end{pmatrix}\ D(1,0)=\begin{pmatrix}D_{xx}(1,0) & D_{xy}(1,0)\\ D_{yx}(1,0) & D_{yy}(1,0)\end{pmatrix}$$

$$D(0,1)=\begin{pmatrix}D_{xx}(0,1) & D_{xy}(0,1)\\ D_{yx}(0,1) & D_{yy}(0,1)\end{pmatrix}\ D(1,1)=\begin{pmatrix}D_{xx}(1,1) & D_{xy}(1,1)\\ D_{yx}(1,1) & D_{yy}(1,1)\end{pmatrix}$$

The elements of dynamical matrix are defined as

$$D_{\alpha\beta}\left(\frac{kk'}{q}\right)=\sum_{l'}\Phi_{\alpha\beta}(l'-l;kk')exp\,(iq.r(lk,l'k')$$

The above equation in matrix form is solved by Python program. And the result is obtained along hexagonal Brillouin zone with symmetry points Γ (0,0). $M(0,\frac{2\pi}{a\sqrt{3}})$ and $K(2\pi/3a,\frac{2\pi}{a\sqrt{3}})$.

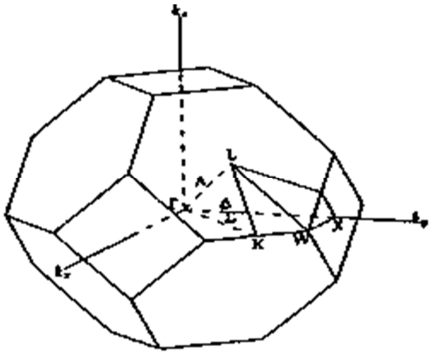

The dispersion relations along symmetry line with coupling constant $\gamma_{j\ =8.4\ x\ 10^{-3}}\gamma$ for stanene is

Γ –M

$$\omega_1^2=\ \gamma_j\left[1-\cos\left(\frac{\sqrt{3}}{2}q_y a\right)\right]$$

$$\omega_2^2=3\,\gamma_j\left[1-\cos\left(\frac{\sqrt{3}}{2}q_y a\right)\right] \quad (5)$$

Along *M–K* are

$$\omega_1^2=3\,\gamma_j\left[1+\cos\left(\frac{q_x a}{2}\right)\right]$$

$$\omega_2^2=\ \gamma_j\left[3-2\cos(q_x a)+\cos\left(\frac{q_x a}{2}\right)\right] \quad (6)$$

Calculated phonon frequencies (cm^{-1}) for Stanene.

Table 1. *Phonon Frequencies For Various Branches.*

Symmetry direction	Acoustical branch		Optical branch	
	Longitudinal	Transverse	Longitudinal	Transverse
q, 0, 0				
0.2, 0, 0	03.636	26.664	179.376	175.740
0.4,0, 0	12.120	48.480	178.164	174.528
0.6,0, 0	20.604	53.328	169.680	173.316
0.8,0, 0	25.452	44.844	160.000	173.316
1, 0, 0	30.300	40.000	147.864	173.316
q, q, 0				
0.2,0.2, 0	30.300	38.784	146.652	173.316
0.4,0.4, 0	36.360	41.208	145.440	170.892
0.6,0.6,0	39.996	43.632	144.228	169.680
0.8,0.8, 0	41.208	48.480	143.016	168.468
1, 1, 0	42.420	49.692	136.956	133.044
q, q, q				
0.2,0.2, 0.2	47.268	39.996	123.624	168.468
0.4,0.4, 0.4	46.056	41.208	110.292	172.104
0.6,0.6, 0.6	48.480	27.876	103.020	175.740
0.8,0.8, 0.8	32.724	18.180	106.656	179.376

And along K–*Γ* are

$$\omega_1^2=\omega_2^2=\ \gamma_j\left[3-\cos(q_x a)-2\cos\left(\frac{q_x a}{2}\right)\cos\left(\frac{\sqrt{3}}{2}q_y a\right)+\sqrt{\left(\cos\frac{q_x a}{2}\cos\frac{\sqrt{3}}{2}q_y a\right)^2+3\sin^2\left(\frac{k_x a}{2}\right)\sin^2\left(\frac{\sqrt{3}}{2}k_y a\right)}\right] \quad (7)$$

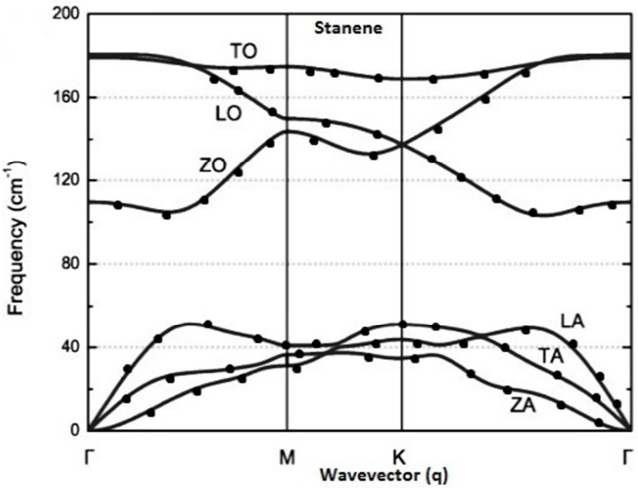

Figure 3. *Phonon frequency along the high symmetry direction Γ-M-K-Γ for stanene.*

3. Phonon Dispersion Curve

The phonon dispersion relations have been computed by

solving the secular equation for the six vibration frequencies corresponding to the phonon wave vectors along the principal symmetry direction *Γ- M- K*.

The phonon dispersion curves have been obtained by plotting these vibration frequencies (ω) against the wave vector ($\vec{q}$) and following points are inferred from the careful analysis of phonon dispersion curve of stanene. The dispersion of the longitudinal phonon exhibits oscillatory behavior extending to the large wave vector transfer region. In contrast, the *ω -q* curves for transverse phonons the oscillatory behavior seems quite insignificant for higher q value. This indicates that the transverse phonons undergo large thermal modulation than do the longitudinal phonon, due to the anharnionicity of atomic vibration at room temperature. The ω -q curves for transverse phonons attain maxima at a higher q value that the longitudinal phonon curves. Figure 3 shows the calculated phonon dispersions of stanene which is in agreement with previous work [15, 16, 17]. Similar to other 2D materials [14], the longitudinal acoustic (LA) and transverse acoustic (TA) branches of group-IV materials are linear near the Γ point Three body interactions have influenced LO and TO branches much more than the acoustic branches LA and TA in this group IV semiconductor 2D material. For wave vectors along the [qq0] and [qqq] symmetry directions the LA and TA modes are both degenerate. There is apparent near-crossing, called anti-crossing of the LO and TO modes along the [q00], and of the LA and TA modes, is also seen for the dispersion curves along [qqq]. This phenomenon is dominant in Stanene. In high symmetry situations, it is possible to separate LO modes from TO modes. The main feature to note is that there is a separation of optic and acoustic mode frequencies across the range of wave vectors; this is because of association of optical vibrations with electric moments. The transverse modes do indeed show a separation of the optic and acoustic modes but there is a crossing of LA & TA modes at 38.788 cm^{-1} and 44.848 cm^{-1}. Optical vibrations are important chiefly in the stanene owing to the strong electric moments associated with motion. Lattice vibrations with wave vector [q00] are showing LO modes moving in opposite directions parallel to [q00], and the TO modes moving in opposite directions perpendicular to [q00]. At [000], the both types of motion become exactly equivalent, in this case LO and TO frequencies would be equal at 178.182 cm^{-1}&173.333 cm^{-1}. But as shifting from [000] to [q00], the long-wavelength optic modes generate electric fields that are either parallel or perpendicular to the direction of propagation of the optic mode will have a significant effect on the frequency of the mode. It follows that $\omega_{LO} < \omega_{TO}$. This effect is known as LO/ TO splitting, reflecting the fact at exactly zero wave vector the frequencies are the same. The dispersion relations along symmetry line show the behavior as at M-K point all four branches are non degenerate and at K-Γ point two of the branches are degenerate-M point LO&TO is showing coupling. The LO-TO coupling has two main effects on the phonon dispersion: (i) flattening the TO branch and (ii) stiffening the LO branch. It should be also noticed that the TA branch (highest acoustic phonon branch at the K point) remains the same with or without the LO-TO coupling, which is similar to the LO branch.

4. Phonon Density of States

We can now derive the density of states for two dimensions.

$$g_j(\omega_j) = \frac{L^2}{\pi}\frac{\omega_j}{v_s^2}$$

here

J=1,2,3,,4,5,6

Where the group velocity is define as

$$v_s = \frac{d\omega_j}{dq_j}$$

Again

$$q_j = q_x, q_x$$

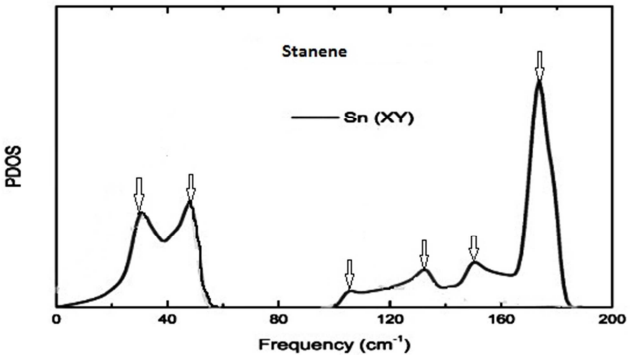

Figure 4. *Projected PDOS for the XY stanene.*

Initially all peaks are absent in the vibrational spectrum. One observes that LA and TO peaks along with other two extra broad peaks LO and TA modes start appearing and finally became quite sharp with large size of atoms. An interesting feature observed in calculated phonon DOS is that, in general, there are six peaks, three each in the acoustic and optical regions. These peaks correspond to the transverse and longitudinal phonons near the Brillouin zone boundary. With the increase of size of the Sn matrix, it is observed that the transverse modes emerge out. They are absent in the DOS for smaller size. The TA and LA modes are extremely sensitive to the values of q_x,q_y. The TO and LO modes depend upon the topology of the cluster and therefore, are absent in smaller size. It is observed that salient features of the phonon density of states of the Stanene are due to short range order and the peak corresponding to the transverse modes are due to the hexagonal nature of semiconductors. The LO and TA are well reproduced with small size of atoms and resemble the features of a IV group 2D semiconductor material like Stanene, where the LO and LA modes improve with the increase of the size of the group of the atoms. The DOS for larger size of atoms are in good agreement with the phonon DOS of crystalline Sn [16, 18]. on the other hand, the DOS is relatively smooth for small size of atoms. The six peaks are 28.696 cm^{-1}, 46.957 cm^{-1}, 104.348 cm^{-1}, 132.174 cm^{-1}, 150.435 cm^{-1}, 172.174cm^{-1}. Here six curves also indicate the group velocity corresponding to six phonon branches [Figure 4].

5. Conclusion

Two-dimensional (2D) materials are one of the most active areas of nanomaterials research due to their potential for integration into next-generation electronic and energy conversion devices. The use of phenomenological models in the study of the vibrational properties of Stanene allows a complete and straightforward description of the phonon dispersion and phonon eigenvectors in the whole Brillouin Zone (BZ) with clear physical ingredients and a small computational effort. Dispersion relation of a material is of great importance in predicting its electronic structure, elastic behavior, thermal properties and optical properties, it becomes quit important in low dimension systems such as nanostructure because in low dimensional systems, understanding of propagation of phonon is of quit important as it is responsible for change in various physical properties. Here in this paper, phonon properties of stanene is compared with others researchers. The theoretical predictions achieved for the phonon dispersion of Stanene are in reasonably good agreement with other researchers. The inclusion of van der Waals interaction (vWI)[5] have influenced both longitudinal and transverse optic modes much more than acoustic branches. The agreement between theory and experimental data at X point is also excellent. Another striking feature of the present model is noteworthy from the excellent reproduction of almost all branches. The computed phonon dispersion curves displayed in Figure 3 show that the inclusion of zero-point energy has improved the results. Since no experimental values on these properties have been reported so far, we are unable to comment as such on the reliability of our results.

In this paper we have systematically reported phonon dispersion curves, combined density of states, of Stanene. On the basis of overall fair agreement, it may be concluded that the present model, three type of Interactions (i) Coulomb interactions (ii) Short range central force Interactions and (iii) a rotationally invariant Keating type bond bending Interaction depending on angle is adequately capable to describe the lattice dynamics of Stanene [15-18].

Acknowledgements

The authors are grateful to the computer centre, S. N. C, Azamgarh for computational assistance. They are also indebted to Prof. R. S. Singh, DDU Gorakhpur university, for many useful discussions.

References

[1] A. C. Ferrari, F. Bonaccorso, V. Fal'Ko, K. S. Novoselov, S. Roche, P. Bøggild, S. Borini, F. H. Koppens, V. Palermo, N. Pugno, and et al., Nanoscale 7, 4598 (2015).

[2] K. S. Novoselov, V. I. Fal'ko, L. Colombo, P. R. Gellert, M. G. Schwab, and K. Kim, Nature 490, 192 (2012).

[3] W. Weber, Adiabatic bond charge model for phonons in diamond, Si, Ge and α- Sn Phys. Rev. B15, 4789 (1977).

[4] K. C Rustagi and Weber, adiabatic bond charge model for phonons in A3B5 Semiconductors, Sol. Stat.-comm. 18,673 (1976).

[5] M. I. Aziz, Ph.D Thesis, V. B. S. P. U, Jaunpur (2010).

[6] R. K. Singh, Physics Reports (Netherland) 85, 259, (1982).

[7] A. A. Maradudin, E. W. Montroll, G. H. Weiss, and I. P. Ipatova, Theory of Lattice Dynamics in the Harmonic Approximation, Solid State Physics, Vol. 3, Eds. H. Ehrenreich, F. Seitz, and D. Turnbull, Academic Press, New York (1971).

[8] P. BruÈesch, Phonons: Theory and Experiments I (Lattice Dynamics and Models of Interatomic Forces), Springer Ser. Solid State Sci. Vol. 34, Eds. M. Cardona, P. Fulde, and H.-J. Queisser, Springer-Verlag, Berlin/Heidelberg/New York (1982).

[9] Hepplestone S P and Srivastava G P, Lattice dynamics of ultrasmall silicon nanostructures Appl. Phys. Lett. 87 231906, (2005).

[10] Hepplestone S P and Srivastava G P, Lattice dynamics of silicon nanostructures, Nanotechnology, 17, 3288–98, (2006).

[11] Seymur Cahangirov, Hasan Sahin, Guy Le Lay and Angel Rubio Introduction to the Physics of Silicene and other 2D Materials, Springer, (2016).

[12] M. Maniraj, B. Stadtmüller, D. Jungkenn, M. Düvel, S. Emmerich, W. Shi, J. Stöckl, L. Lyu, J. Kollamana, Z. Wei, A. Jurenkow, S. Jakobs, B. Yan, S. Steil, M. Cinchetti, S. Mathias & M. Aeschlimann, Communications Physics, 2, Article number: 12 (2019).

[13] Sumit Saxena, Raghvendra Pratap Chaudhary & Shobha Shukla Scientific Reports, 6, 31073 (2016).

[14] Gour P. Dasa, Parul R. Raghuvanshi, Amrita Bhattacharya, 9th International Conference on Materials Structure and Micromechanics of Fracture Phonons and lattice thermal conductivities of graphene family, 23, 334-341, (2019).

[15] Md. Habibur Rahman, Md Shahriar Islam, Md Saniul Islam, Emdadul Haque Chowdhury, Pritom Bose, Rahul Jayan and Md Mahbubul Islam, Physical Chemistry Chemical Physics, 23, 11028-11038, 2021.

[16] Novel Lattice Thermal Transport in Stanene Bo Peng, Hao Zhang, Hezhu Shao, Yuchen Xu, Xiangchao Zhang and Heyuan Zhu, Scientific Reports, August 2015.

[17] Wu, Liyuan; Lu, Pengfei; Bi, Jingyun; Yang, Chuanghua; Song, Yuxin; Guan, Pengfei; Wang, Shumin, Nanoscale Research Letters, volume 11, 525 (2016).

[18] Bo Peng, Hao Zhang, Hezhu Shao, Yuanfeng Xu, Gang Ni, Rongjun Zhang, and Heyuan Zhu, Phys. Rev. B 94, 245420 (2016).